

responds to a flattened-tetrahedral configuration of copper(II) with D_{2d} symmetry.

Minor solvation for the anions than for the cations is remarkably confirmed in the unsolvated CuCl_4^{2-} species; similarity of the CT and d-d transition bands in all solvents is quantitatively described.

Summary

Copper(II) complexation by the chloride ion was investigated in trimethyl phosphate solutions, and quantitative conclusions upon the stability and the electronic spectra of CuCl^+ , CuCl_2 , CuCl_3^- , and CuCl_4^{2-} were obtained by using an original calculation method for spectrophotometric data.

The solvent effect on the stability, the electronic spectra, and the structure of copper(II) chloro complexes is discussed for the [1,2,3,4] model in six aprotic dipolar solvents. A good correlation with the solid-state results is obtained in the absorption bands assignment and in the copper(II) configuration, especially for the tetrachloro complex.

The stabilization of the chlorocuprates in solution is an inverse function of the solvent donor numbers (Table II). This effect increases with higher coordination of chloride atoms to copper(II). Complexes are less stable in better solvating solvents: this well-known property is verified quantitatively for the first time for successive mononuclear complexes identified in a large set of aprotic solvents.

The calculated electronic spectra provide the possibility to classify the chlorocuprates into two groups, the first one containing cationic and neutral species, i.e. uncomplexed copper(II) mono-

and dichloro complexes, and the second one the anionic species, i.e. the tri- and tetrachloro complexes.

(i) The first group species have two main absorption bands, in the UV region between 260 and 310 nm and in the near-IR region between 790 and 1000 nm. Little shifts of the CT bands, where uncomplexed copper(II) is progressively substituted to CuCl_2 , are observed but do not correlate with macroscopic properties of the solvents; however, regular bathochromic shifts of the d-d transition bands define for the crystal field parameter Dq an original sequence:



(ii) The electronic spectra variations of the anionic species are less solvent-dependent: this confirms the fact that, in the solvents under investigation, the solvation is less important for the anions than for the cations.²⁵ This property is very well satisfied for the unsolvated CuCl_4^{2-} ion for which the CT and d-d transition bands are remarkably solvent-independent.

(iii) When the ligand concentration increases, the bathochromic shifts of the d-d transition bands indicate configuration changes of copper(II): the structure is square planar for the cationic and neutral complexes and becomes flattened tetrahedral for the tetrachloro complex.

Registry No. Trimethyl phosphate, 512-56-1.

Supplementary Material Available: Complete electronic spectra (CT and d-d transition bands) of uncomplexed copper(II) (Figure 4) and individual copper(II) chloro complexes (Figures 5-8) calculated in six aprotic solvents and absorption maxima coordinates (Tables III-VII) (8 pages). Ordering information is given on any current masthead page.

Contribution from the Department of Physical Chemistry, Hebrew University of Jerusalem, Jerusalem 91904, Israel, and Department of Chemistry, Princeton University, Princeton, New Jersey 08544

Bonding in Zinc Proto- and Mesoporphyrin Substituted Myoglobin and Model Compounds Studied by Resonance Raman Spectroscopy

Jehuda Feitelson[†] and Thomas G. Spiro*[‡]

Received September 24, 1985

Resonance Raman spectra are reported for myoglobin reconstituted with zinc protoporphyrin and mesoporphyrin and for imidazole complexes of zinc protoporphyrin in methylene chloride. The bands are assigned with reference to previous studies of iron protoporphyrin and mesoporphyrin complexes. Coordination of zinc protoporphyrin by imidazole produces a downshift of the porphyrin core size marker frequencies, consistent with the core size expansion observed in five-coordinate zinc porphyrin crystal structures. The five-coordinate frequencies are observed for zinc myoglobin, implying coordination by the proximal histidine residue. The zinc-imidazole bond stretching frequency has been detected in the low-frequency region of the spectra, at 190, 183, and 177 cm^{-1} , for zinc protoporphyrin adducts with imidazole, 4-methylimidazole, and 2-methylimidazole, respectively. The 6- cm^{-1} difference between the last two values is an expression of the steric influence of the 2-methylimidazole ligand. All of these values are significantly below those observed for iron(II) protoporphyrin, implying a significantly weaker bond from imidazole to zinc than to iron. The proteins show a much weaker zinc-imidazole band, at a lower frequency, 148 cm^{-1} . Thus the zinc-imidazole bond in the myoglobin samples appears to be significantly weaker than normal zinc-imidazole bonds, presumably due to geometric constraints in the heme binding pocket.

Introduction

The substitution in metalloenzymes of metals other than the one contained in the native protein provides an opportunity to test the flexibility and restraints of the protein environment in the metal binding pocket. In this study we use zinc proto- and mesoporphyrin as probes of the heme binding pocket of myoglobin (Mb). This oxygen carrier contains iron(II) protoporphyrin in a cavity with a number of noncovalent contacts, the iron ion being coordinated by the imidazole side chain of the proximal histidine, His-93. There is also a distal histidine (His-64) whose imidazole residue is too far to coordinate to the iron but is in a position to

form an H-bond to the outer atom of bound dioxygen.

The heme group is readily extracted from Mb and can be replaced by a variety of metalloporphyrins.¹ In this study we have reconstituted apo-Mb with ZnPP (PP = protoporphyrin IX) and ZnMP (MP = mesoporphyrin IX) and have examined the resonance Raman (RR) spectra of these artificial zinc proteins, as well as of imidazole adducts of zinc protoporphyrin IX dimethyl ester (ZnPPDME) in CH_2Cl_2 solution. The resonance Raman bands of iron porphyrin complexes and of native Mb have been studied extensively.²⁻⁴ The higher frequency porphyrin skeletal

* To whom correspondence should be addressed.

[†] Hebrew University of Jerusalem.

[‡] Princeton University.

(1) Leonard, J. J.; Yonetani, T.; Callis, J. B. *Biochemistry* **1974**, *13*, 1460-1464.

(2) Choi, S.; Spiro, T. G.; Langry, K. C.; Smith, K. M.; Budd, D. L.; LeMar, G. M. *J. Am. Chem. Soc.* **1982**, *104*, 4345-4351.

(3) Choi, S.; Spiro, T. G. *J. Am. Chem. Soc.* **1983**, *105*, 3683.

modes are sensitive to the nature of the axial ligands via their effect on the geometric and electronic structure.⁴⁻⁶ In addition the metal-axial ligand stretching vibrations can sometimes be located in the low-frequency RR spectra, which also contain in- and out-of-plane deformation modes of the porphyrin macrocycle and its peripheral substituents.³ These spectral features are useful in assessing the nature of the ligation in zinc myoglobin. They permit us to conclude that while the proximal histidine does coordinate to the zinc, the zinc-imidazole bond is anomalously weak. It appears that the orientation of the proximal histidine is suboptimal for binding to the zinc and that it is held relatively rigidly in the heme pocket.

Experimental Section

ZnPPDME was obtained from Mid Century (Posen, IL), and ZnPPIX and ZnMPIX were from Porphyrin Products (Logan, UT). Imidazole (ImH), 2-methylimidazole (2MeImH), and 4-methylimidazole (4MeImH) from Sigma were purified by sublimation. CH₂Cl₂ was a Mallinckrodt SpectrAR product. Doubly distilled water was used throughout. Solutions of ZnPPDME in CH₂Cl₂ for resonance Raman measurements were 1 mM in porphyrin and about 8 mM in the imidazole derivatives.

Lyophilized sperm whale myoglobin (Sigma) was purified by isoelectric focusing electrophoresis. It was extracted from the agarose gel with a minimal amount of water and the gel spun off in a refrigerated Sorvall centrifuge at 18 000 rpm and 4 °C. The solution was dialyzed overnight against water at 4 °C.

The apomyoglobin was prepared by the butanone method.⁷ Since apomyoglobin is very heat sensitive, its preparation and subsequent reconstitution were carried out in the cold room (~4 °C). All solutions were precooled and whenever possible kept in an ice bath. The myoglobin was acidified with 0.1 N HCl to pH 4.3 and shaken in a separating funnel with an equal volume of cold 2-butanone. After it was separated from the deeply colored heme-containing phase, the lightly colored aqueous apomyoglobin was dialyzed at 2-4 °C against water. Its concentration was determined spectrophotometrically at 280 nm with the use of $\epsilon_{280} = 1.58 \times 10^4 \text{ m}^{-1} \text{ cm}^{-1}$. The protein was reconstituted with ZnPP or with ZnMP by a procedure similar to that of Scholler et al.⁸ Typically 11 μmol of ZnPP or ZnMP was wetted with 2 drops of pyridine, dissolved in ~0.5 mL of 0.1 N NH₄OH, and diluted to 2 mL with water. The pH of a solution containing about 10 μmol of apomyoglobin was adjusted to pH 8.6 and the porphyrin solution was added dropwise with shaking. The pH was readjusted to pH ~8.6 and the solution left in the ice bath for about 30 min. The pH was lowered to pH 7 with 0.1 N HCl and the solution loaded onto a CM-52 column that had been equilibrated with 0.01 M phosphate buffer, pH 7.0. After the elution was begun with about 5 column volumes of the above buffer, the protein was eluted as a sharp band with 0.25 M phosphate buffer, pH 7.0. The pink eluate was concentrated by forcing part of the solvent through an Amicon ultrafiltration membrane and divided into 300- μL aliquots in plastic minivials, which were deep-frozen in liquid N₂. Subsequently one vial was thawed and used for each experiment. All work with the light-sensitive ZnPP was carried out in the dark. When necessary a dim dark red light was used briefly. The concentrations of the reconstituted ZnPP- and ZnMP-myoglobins were determined from their porphyrin absorbances. The final solution concentrations were about 0.2 mM.

For resonance Raman scattering measurements at room temperature the solutions were deoxygenated in NMR tubes capped with rubber septum caps. The ZnPPDME solutions were bubbled with N₂. The protein solutions were flushed with N₂ without bubbling. The procedure of Walters and Spiro⁹ was used for room-temperature RR measurements. The low-temperature measurements were carried out in a cryostat described by Czernuszewicz et al.¹⁰

Solutions were checked for their stability before and after illumination since extensive exposure to the laser light caused their deterioration. Only experiments where no spectral change was observed were retained.

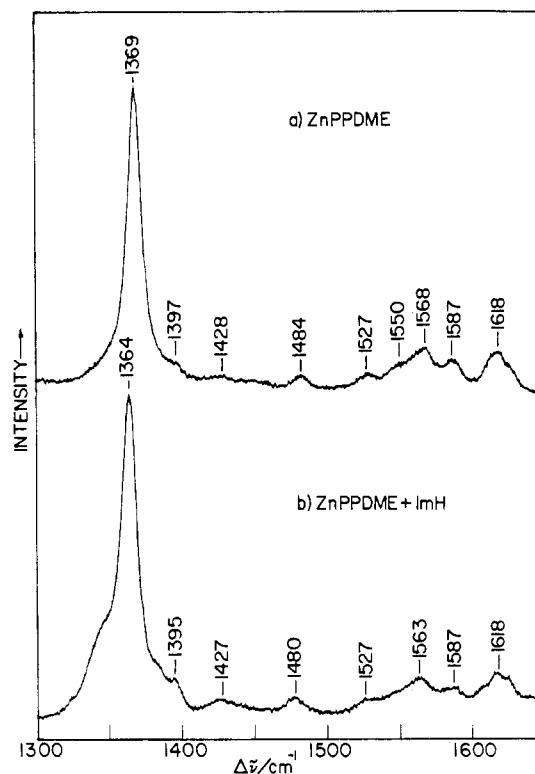


Figure 1. Raman spectra of 1 mM ZnPPDME in CH₂Cl₂ in (a) the absence and (b) the presence of 8 mM ImH ($\gamma_{\text{exc}} = 4131 \text{ \AA}$, 70-mW power, 5-cm⁻¹ bandwidth, 0.5 cm⁻¹/s scan rate, 3 scans, 1300-1700 cm⁻¹).

Table I. Frequencies (cm⁻¹) and Assignments for Aqueous Reconstituted Mb and for Model Complexes in CH₂Cl₂^a

	ZnPPDME	(ImH)- ZnPPDME	Mb- (ZnPP)	Mb- (ZnMP)
$\nu(\text{C}=\text{C})^b$	1618	1618	1617	
ν_{37}	1587	(1587)	1584	1589
ν_2	1568	1563	1564	(1570)
ν_{38}	1527	(1527)		
ν_{11}	(1550)		(1545)	
ν_3	1484	1480	1481	(1478)
$\delta_s(\text{=CH}_2)$	(1428)	1427	1426	
ν_{20}, ν_{29}	(1397)	1395	(1389)	1395
ν_4	1369	1364	1364	1365
vinyl bend ^c	408	409	408	
pyr fold			400	390
$2 \nu_{35}$	366	366	374	364
ν_8	344	345	342	340
vinyl bend	309	310	305	
ν_9	265	263	272	275
pyr tilt			246	257
$\nu(\text{Zn}-\text{ImH})$		190 ^d	148	149

^a All at room temperature; values in parentheses are uncertain due to weakness and/or breadth of the bands. ^b See ref 2 for assignments. ^c See ref 3 for assignments. ^d 183 and 177 cm⁻¹ for 4-MeImH and 2-MeImH adducts.

The Kr⁺ ion laser line at 413.1 nm was used for excitation of zinc protoporphyrin IX dimethyl ester and ZnPPMb. Because of the missing vinyl groups the ZnMP Soret band is blue shifted by 12 nm with respect to ZnPP. The 406.7-nm laser line was therefore used for ZnMPMb excitation.

Absorption spectra were measured on a Hewlett-Packard 8450 diode array spectrophotometer.

Results and Discussion

High-Frequency Modes: Core Expansion. Figure 1 shows resonance Raman spectra in the 1300-1700-cm⁻¹ region for 1 mM zinc protoporphyrin dimethyl ester (ZnPPDME) in CH₂Cl₂ solution in the presence and absence of 8 mM imidazole (ImH), with 413.1-nm excitation, in resonance with the B (Soret) band. Zinc porphyrins fluoresce strongly, but the emission is from the lower

- (4) Spiro, T. G. In "Iron Porphyrins"; Lever, A. B. P., Gray, H. B., Eds.; Addison-Wesley: Reading, MA, 1983; Part 2, pp 89-159.
- (5) Scheidt, W. R.; Kastner, M. E.; Hatano, K. *Inorg. Chem.* **1978**, *17*, 706-710.
- (6) Nappa, M.; Valentine, J. S. *J. Am. Chem. Soc.* **1978**, *100*, 5075-5080.
- (7) Teale, F. W. J. *Biochim. Biophys. Acta* **1959**, *35*, 543.
- (8) Scholler, D. M.; Wang, M. R.; Hoffman, B. *Methods Enzymol.* **1981**, *76*, 487-493.
- (9) Walters, M. A.; Spiro, T. G. *Biochemistry* **1983**, *21*, 6989-6995.
- (10) Czernuszewicz, R. S.; Johnson, M. K. *Appl. Spectrosc.* **1983**, *37*, 297-298.

energy excited state, associated with the Q band, and the emission background near the Soret band is negligible. At longer wavelengths the fluorescence interferes, however, and RR spectra with Q-band excitation cannot be obtained. These spectra resemble those of iron(II) protoporphyrin complexes² and can be assigned with reference to the latter, as shown in Table I. The RR bands that are enhanced via the Soret transition include the totally symmetric porphyrin skeletal modes,⁴ especially ν_4 , the primarily C-N breathing mode¹¹ at 1369–1364 cm^{-1} , which dominates the spectra. The other totally symmetric modes, ν_2 and ν_3 at 1568–1563 and 1484–1480 cm^{-1} , are substantially weaker. In addition, the vinyl peripheral substituents, which are conjugated with the ring, introduce modes in this region:¹² the C=C stretching band at 1618 cm^{-1} and a =CH₂ scissors mode at 1428 cm^{-1} . The asymmetric disposition of the vinyl substituents also induces Raman activity into E_u-type (infrared) skeletal modes, ν_{37} at 1587 cm^{-1} and ν_{38} at 1527 cm^{-1} .¹² Finally, weak non totally symmetric porphyrin skeletal modes can be seen as shoulders at $\sim 1550 \text{ cm}^{-1}$ (ν_{11}) and $\sim 1397 \text{ cm}^{-1}$ (ν_{20} and ν_{29}).

The protoporphyrin skeletal modes above 1450 cm^{-1} are sensitive to the core size of the porphyrin (defined as C₁-N, the distance from the center of the ring to the pyrrole N atoms), as determined by the properties of the central metal ion and the axial ligands. For a series of iron and nickel protoporphyrin complexes the frequencies were found to follow the empirical equation $\nu = K(A - d)$, where d is the C₁-N distance and K and A are parameters for each of the skeletal modes.² Applying these parameters to ZnPP, and assuming it has the same core size as ZnTPP (TPP = tetraphenylporphine), for which $d = 2.036 \text{ \AA}$,⁵ gives frequencies in remarkably good agreement with experiment. The predicted values $\nu_{37} = 1584 \text{ cm}^{-1}$, $\nu_2 = 1561 \text{ cm}^{-1}$, $\nu_{11} = 1550 \text{ cm}^{-1}$, $\nu_{38} = 1525$, $\nu_3 = 1486 \text{ cm}^{-1}$ are all within 3 cm^{-1} of the observed frequencies, except for ν_2 , which is 6 cm^{-1} low. However, the ν_2 band overlaps ν_{11} in the RR spectra, and it is likely that proper band resolution would lower the measured frequency and bring it into better agreement with the calculated value. In addition ν_{10} is calculated at 1616 cm^{-1} , under the $\nu_{\text{C}=\text{C}}$ band, thereby explaining the absence of an assignable ν_{10} band in the spectrum. Likewise ν_{19} is predicted at 1564 cm^{-1} , overlapping the ν_2 band; being an A_{2g} mode it is not in any event expected to be enhanced significantly with Soret excitation.⁴ The only other missing skeletal mode is ν_{28} (B_{2g}) expected at 1450 cm^{-1} , which also is not enhanced with Soret excitation. In heme complexes the ν_4 mode is responsive to the Fe oxidation state and to electronic properties of the porphyrin,⁴ but there is also an underlying core size dependence.¹³ The predicted²⁶ value for ν_4 is 1371 cm^{-1} , only 2 cm^{-1} higher than observed.

When imidazole is bound to ZnPPDME, the ν_2 and ν_3 frequencies decreased by 4–5 cm^{-1} (Figure 1 and Table I). This is consistent with the larger core size, 2.045 Å on average, for five-coordinate Zn porphyrin complexes.⁵ Binding of an axial ligand results in movement of the Zn atom 0.33 Å , on average, out of the porphyrin plane toward the ligand. While this motion might have been expected to relax the core size toward its preferred value of $\sim 2.01 \text{ Å}$,¹⁴ this effect is apparently overridden by the nonbonded interactions between the pyrrole N atoms and the axial ligand, which force the core to expand.^{15,16} The 0.01- Å expansion is predicted² to decrease all the skeletal mode frequencies above 1450 cm^{-1} by 4–5 cm^{-1} , in excellent agreement with the observed shifts of ν_2 and ν_3 . While ν_{37} and ν_{38} seem not to shift as they should, the bands are too weak to be certain about this. The core size dependence of ν_4 is weaker, and only a 2- cm^{-1} downshift is expected,²⁶ whereas a 5- cm^{-1} shift is clearly seen on imidazole

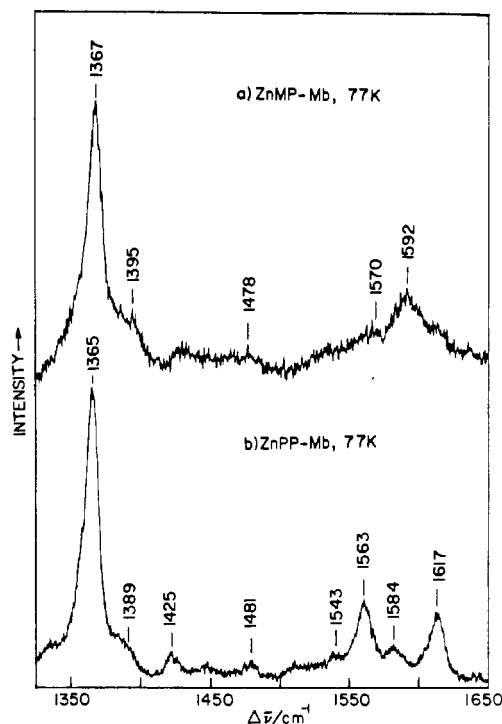


Figure 2. Raman spectra of (a) aqueous ZnMP-Mb at 77 K excited at 4067 Å and (b) aqueous ZnPP-Mb at 77 K excited at 4131 Å (50-mW power, 6- cm^{-1} bandwidth, 0.5 cm^{-1}/s scan rate, 2 scans).

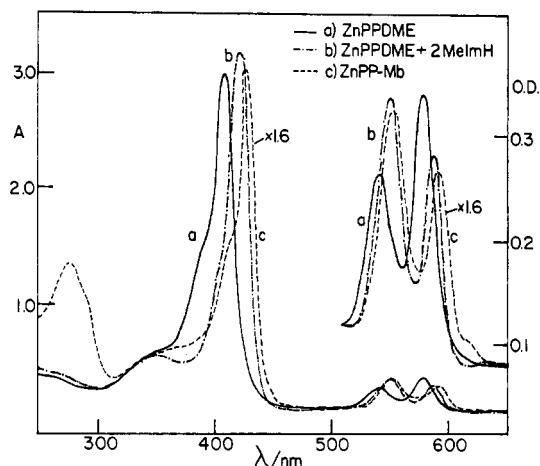


Figure 3. Absorption spectra of (a) 0.22 mM ZnPPDME in CH_2Cl_2 , (b) 0.22 mM ZnPPDME in the presence of 1.5 mM 2-MeImH in CH_2Cl_2 , and (c) ZnPP-Mb in aqueous solution.

binding. The extra shift may be due to doming of the porphyrin, the tendency of the pyrrole rings to tilt, in five-coordinate complexes, in order to allow the N atoms to follow the out-of-plane movement of the metal atom.¹⁷ Doming was invoked to explain the much larger deviation (12 cm^{-1}), from the core-size prediction, for the deoxyMb model complex (2-MeImH)Fe^{II}PP,¹³ pronounced doming is seen in the crystal structure of (2-MeImH)Fe^{II}TPP.¹⁸ If this view is correct, only modest doming is required to explain the extra downshift of ν_4 for the ZnPP imidazole adduct, consistent with the crystal structures of five-coordinate Zn porphyrins.^{3,5}

Figure 2 shows RR spectra in frozen aqueous solution for Mb reconstituted with ZnPP, excited at 413.1 nm, and for Mb reconstituted with ZnMP, excited at 406.7 nm. Spectra obtained at room temperature showed very similar band frequencies, differing at most by 2 cm^{-1} , but were less well resolved. The

(11) Abe, M.; Kitagawa, T.; Kyogoku, Y. *J. Chem. Phys.* **1978**, *69*, 4526.

(12) Choi, S.; Spiro, T. G.; Langry, K. C.; Smith, K. M.; *J. Am. Chem. Soc.* **1982**, *104*, 4337–4344.

(13) Spiro, T. G. *Adv. Protein Chem.* **1985**, *37*, 110–159.

(14) Hoard, J. L., In "Porphyrins and Metalloporphyrins"; Smith, K. M., Ed.; Elsevier: New York, 1975; pp 317–376.

(15) Olafson, B. D.; Goddard, W. A. *Proc. Natl. Acad. Sci. U.S.A.* **1977**, *74*, 1315.

(16) Warschel, A. *Proc. Natl. Acad. Sci. U.S.A.* **1977**, *74*, 1789.

(17) Spiro, T. G.; Stong, J. D.; Stein, P. *J. Am. Chem. Soc.* **1979**, *101*, 2648–2655.

(18) Hoard, J. L.; Scheidt, W. R. *Proc. Natl. Acad. Sci. U.S.A.* **1973**, *73*, 919; **1974**, *71*, 1578.

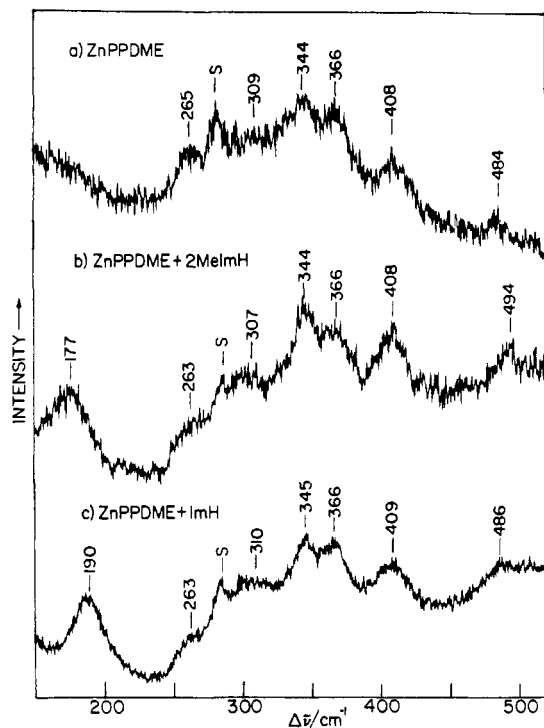


Figure 4. Raman spectra of 1 mM ZnPPDME in CH_2Cl_2 , (a) in the absence of imidazole derivative, (b) in the presence of 8 mM 2MeImH, and (c) in the presence of 8 mM ImH ($\gamma_{\text{exc}} = 4131 \text{ \AA}$, 70-mW power, 5- cm^{-1} bandwidth, 0.5 cm^{-1}/s scan rate, 3 scans).

room-temperature frequencies are presented in Table I. The frequencies for the protein sample containing ZnPP are the same as those of the imidazole adduct of ZnPPDME in CH_2Cl_2 , implying that the Zn is coordinated by the proximal histidine in the protein. This inference is supported by the visible absorption spectra, shown in Figure 3. Addition of imidazole to ZnPP produces distinct absorption changes, as noted by Korleva et al.¹⁹ The absorption spectrum of ZnMb agrees with that of the ZnPP imidazole adduct.

There are some RR intensity differences between protein and model. In particular, the vinyl C=C stretch and the ν_2 mode seem to be more strongly enhanced in the protein, relative to the non totally symmetric skeletal modes. The protein substituted with ZnMP shows spectral differences which are expected because of the replacement of the peripheral vinyl groups with ethyl groups.¹² There are, of course, no vinyl modes, nor are the E_u -type modes activated by the ethyl groups. Nevertheless, a weak band can be seen at the ν_{37} frequency, and an anomalously strong band is seen at 1592 cm^{-1} , the expected ν_{38} position; evidently the asymmetry of the protein environment is sufficient to produce activation of the E_u -type modes, especially ν_{38} . The ν_2 frequency is $\sim 6 \text{ cm}^{-1}$ higher than in the protoporphyrin derivative, in which it is coupled with the vinyl C=C stretch.¹² The ν_3 , ν_4 , and $\nu_{20,29}$ frequencies are essentially the same in the meso- and protoporphyrin reconstituted proteins.

Low-Frequency Spectra: Zn-Imidazole Stretching. Figure 4 shows 413.1-nm-excited RR spectra in the region below 450 cm^{-1} for ZnPPDME and its adducts with ImH and 2-MeImH, while Figure 5 shows similar spectra for zinc proto- and mesoporphyrin substituted myoglobin. This region contains a number of in- and out-of-plane deformation modes, as well as peripheral vinyl bending modes, which are readily assigned by reference to the iron porphyrin spectra.³ The ZnPP-Mb spectrum looks different from those of the ZnPPDME complexes in methylene chloride, but this is mostly a result of sharpening and intensification of the bands in the protein. Some of the sharpening is due to the low temperature of the frozen protein solution, but the room-temperature

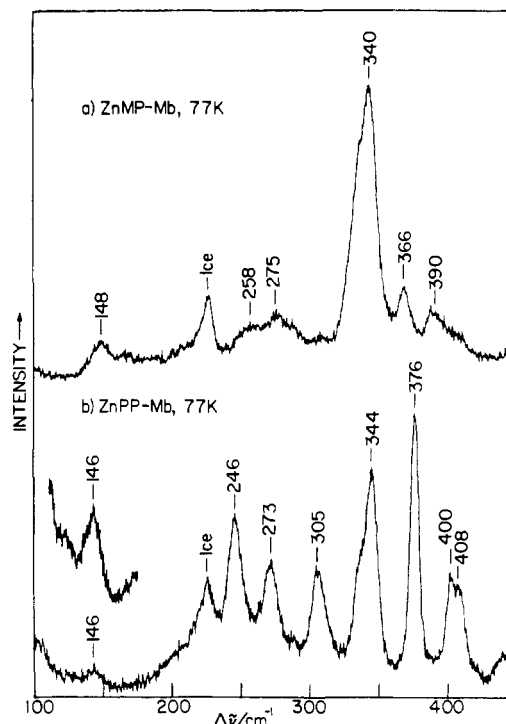


Figure 5. Raman spectra of (a) aqueous ZnMP-Mb at 77 K excited at 4067 \AA and (b) aqueous ZnPP-Mb at 77 K excited at 4131 \AA (50-mW power, 6- cm^{-1} bandwidth, 0.5 cm^{-1}/s scan rate, 2 scans; inset 8 scans).

spectrum is also much better resolved than that of the complexes in CH_2Cl_2 . The breadth of the low-frequency bands in the latter may reflect porphyrin conformational flexibility, to which the low-frequency deformation modes would be sensitive; this flexibility might well be reduced in the protein binding pocket. There are also changes in relative intensity, e.g. the augmentation of the 376- and 246- cm^{-1} bands in ZnPP-Mb, which probably reflect specific protein contacts that alter the porphyrin excited-state potential surface.

While the band frequencies are quite similar (Table I), two of the bands assigned to in-plane deformation modes, ν_8 and $2\nu_{35}$, show 8- cm^{-1} upshifts in the protein relative to those bands for the complexes in solution, possibly reflecting protein constraints on the peripheral substituents, whose deformations provide important contributions to the compositions of these normal modes.¹¹ The spectrum of ZnMP-Mb is dramatically different in appearance, reflecting the importance of the vinyl groups in activating the deformation modes and in contributing two of the bands in this region, associated with vinyl bending.³ In addition the relative intensities of ν_8 and $2\nu_{35}$, which are believed to be involved in a Fermi resonance,¹¹ are very different in the two reconstituted proteins; Fermi doublets do show large changes in relative intensity with relatively small changes in the frequency of the interacting modes.

Near 200 cm^{-1} the spectrum of ZnPPDME in CH_2Cl_2 is blank, but that of the ImH adduct shows a prominent band at 190 cm^{-1} , shifting to 177 cm^{-1} in the spectrum of the 2-MeImH adduct. This sensitivity to the nature of the imidazole establishes this band as the zinc-imidazole stretch, analogous to the Fe-imidazole stretch seen at 220 cm^{-1} in native Mb and in the e range 200–230 cm^{-1} for a variety of imidazole adducts of iron porphyrins.^{20,21} The (4-MeImH)ZnPP adduct gives a band at 183 cm^{-1} . The methylimidazoles are more basic than unsubstituted imidazole due to electron donation from the methyl substituents; this factor, which should strengthen the zinc-imidazole bond, is evidently overridden by the larger mass of the methyl-substituted ligands. 2-MeImH and 4-MeImH have the same mass and essentially the

(19) Kosolava, T. A.; Koifman, O. I.; Beresin, B. D. *Koord. Khim.* **1981**, *7*, 1642–1647.

(20) Stein, P.; Mitchell, M.; Spiro, T. G. *J. Am. Chem. Soc.* **1980**, *102*, 7795–7797.

(21) Hori, H.; Kitagawa, T. *J. Am. Chem. Soc.* **1980**, *102*, 3608–3613.

same basicity. The 6-cm^{-1} difference between them in the zinc-imidazole stretching frequency is attributed primarily to the steric effect of the 2-methyl group, which is expected to have short nonbonded contacts with the pyrrole rings.²²

The reconstituted proteins do not show any band between 175 and 200 cm^{-1} (Figure 5). They both show a weak but well-resolved band at 148 cm^{-1} . This is assigned to the Zn-imidazole stretch in the proteins. It is much weaker and lower in frequency than the Zn-imidazole bands seen in the model complexes. The best reference complex is probably the 4-MeImH adduct, the 4-methyl group mimicking the methylene linkage of the imidazole side chains to the polypeptide backbone in the protein. If the Zn-imidazole stretch is modeled with a diatomic oscillator, with masses 65 (Zn) and 82 (4-MeImH), then the force constant is $0.76\text{ mdyne}/\text{\AA}$ for the 4-methylimidazole adduct but only $0.48\text{ mdyne}/\text{\AA}$ for ZnMb. Thus the Zn-imidazole bond is evidently much weaker in the protein than in the model complexes. This is not the case for native Mb, which shows an imidazole-stretching frequency,^{23,24} 220 cm^{-1} ($k = 1\text{ mdyne}/\text{\AA}$), that is in the range found for model complexes.^{20,21} We conclude that the proximal imidazole is not optimally oriented for binding to Zn in the reconstituted protein.

One factor in differentiating Zn from Fe in the protein is that the out-of-plane displacement of the metal in five-coordinate complexes is 0.33 for Zn^{II} but 0.55 for Fe^{II} .¹⁸ Another factor is that the Zn-imidazole bond is intrinsically weaker than the Fe-imidazole bond. Thus in a non-H-bonding solvent the (2-MeImH)Fe^{II}PP frequency is 207 cm^{-1} ,²⁰ 30 cm^{-1} higher than for (2-MeImH)ZnPP. Consequently, a suboptimal position of the proximal imidazole can be accommodated by lengthening an already weak Zn-imidazole bond. Nevertheless, this phenomenon implies a relatively rigid positioning of the proximal histidine, presumably via the surrounding nonbonded contacts,²⁵ since an $\sim 0.2\text{-\AA}$ movement of a side chain would ordinarily be expected to require very little energy.

Acknowledgment. We thank Roman Czernuszewicz and Niraja Parthasarathi for valuable technical assistance. This work was supported by NIH Grant GM33576.

Registry No. ZnPPDME, 15304-09-3; (ImH)ZnPPDME, 80481-01-2; (2-MeImH)ZnPPDME, 100228-83-9; (4-MeImH)ZnPPDME, 100243-48-9; L-His, 71-00-1.

- (22) Collman, J. P.; Halbert, T. R.; Suslick, K. *Met. Ions Biol.* **1980**, *2*, 1-72.
 (23) Kitagawa, T.; Nagai, K.; Tsubaki, M. *FEBS Lett.* **1979**, *104*, 376.
 (24) Argade, P. V.; Sassaroli, M.; Rousseau, D. L.; Inubeushi, T.; Ikeda-Saito, M.; Lapidot, A. *J. Am. Chem. Soc.* **1984**, *106*, 6593-6596.

- (25) Takano, T. *J. Mol. Biol.* **1977**, *110*, 537-568.
 (26) The parameters K and A for ν_4 were omitted from ref 13, which gave the empirical core size plot. They are $K = 133.3\text{ cm}^{-1}/\text{\AA}$ and $A = 12.32\text{ \AA}$. In support of the use of ZnTPP structure parameters, we note that bond lengths and core size are nearly independent of the porphyrin peripheral substituents for given central metal and axial ligands.¹⁴

Contribution from the Research School of Chemistry,
 Australian National University, Canberra, ACT 2601, Australia

Intramolecular Phosphoryl Transfer: Chelated Phosphoramidate

P. Hendry and A. M. Sargeson*

Received August 20, 1985

2,4-Dinitrophenyl phosphate (DNPP) coordinated to the pentaamminecobalt(III) moiety is rapidly lysed in aqueous base to yield the previously unobserved N,O-chelated phosphoramidate and 2,4-dinitrophenolate (DNP) ions. The chelate ring then opens to monodentate N-bound phosphoramidate. The reaction is almost quantitative (98%) at $5\text{ }^\circ\text{C}$ and obeys the rate law $\nu_{\text{DNP}} = k[\text{CoDNPP}][\text{OH}^-]$ with $k = (1.96 \pm 0.03) \times 10^{-2}\text{ L mol}^{-1}\text{ s}^{-1}$ at $25\text{ }^\circ\text{C}$ and $\mu = 1.0\text{ M}$. With increasing temperature Co-O bond rupture releases increasing amounts of unreacted phosphate ester. The mechanism is argued in terms of a deprotonated ammonia attacking the adjacent P center to give an aminophosphorane, which then decomposes to the chelate phosphoramidate. Subsequent ring opening and phosphoramidate loss are ascribed to the normal conjugate base chemistry of Co(III) amine complexes. The intramolecular substitution of NH_2^- for the phenolate ion at the P center is very rapid compared with analogous chemistry for the uncoordinated ion.

Introduction

The enzymic hydrolysis of phosphates and phosphate esters is remarkable in that many of the known enzymes require at least one divalent metal ion for activity.¹ This observation has stimulated research into the role that metal ions play in both the enzymic and nonenzymic hydrolysis of phosphates.^{1,2} Work in this laboratory has concentrated on the synthesis and hydrolysis of well-defined, substitution-inert metal ion phosphate complexes designed to test the efficacy of certain types of reaction paths for their possible role in enzymic phosphate chemistry.³⁻⁵ In this context, the reactivity of phosphate derivatives in the pentaamminecobalt(III) complexes^{6,7} $[(\text{NH}_3)_5\text{CoOPO}_3\text{C}_6\text{H}_4\text{NO}_2]^+$ and

$[(\text{NH}_3)_5\text{CoOPO}_2\text{F}]^+$ has been studied. In both these cases, it was postulated that reaction proceeded via attack of a cis-coordinated deprotonated ammonia on the phosphorus center to yield a five-coordinate aminophosphorane activated complex, which decayed to a presumed N,O chelate phosphoramidate (Scheme I). The chelate, however, was never observed and was presumed to undergo ring opening rapidly under the conditions in which it was produced.^{6,7} The aim of the present study was to observe the chelate formation and decay. This aim might be achieved by making the precursor complex more reactive, i.e. by improving the leaving-group ability of the ester function in comparison to that used in the previous studies. To this end, the leaving group chosen was 2,4-dinitrophenolate ion since its phosphate ester is well characterized⁸ and is known to be more reactive than 4-

- (1) Morrison, J. F.; Heyde, E. *Annu. Rev. Biochem.* **1972**, *41*, 29.
 (2) Cooperman, B. S. *Met. Ions Biol. Syst.* **1976**, *2*, 79-125.
 (3) Jones, D. R.; Lindoy, L. F.; Sargeson, A. M. *J. Am. Chem. Soc.* **1983**, *105*, 7327.
 (4) Anderson, B.; Milburn, R. M.; Harrowfield, J. M.; Robertson, G. B.; Sargeson, A. M. *J. Am. Chem. Soc.* **1977**, *99*, 2652.
 (5) Hendry, P.; Sargeson, A. M. *J. Chem. Soc., Chem. Commun.* **1984**, 164.

- (6) Harrowfield, J. M.; Jones, D. R.; Lindoy, L. F.; Sargeson, A. M. *J. Am. Chem. Soc.* **1980**, *102*, 7733.
 (7) Creaser, I. I.; Dubs, R. V.; Sargeson, A. M. *Aust. J. Chem.* **1984**, *37*, 1999.
 (8) Ramirez, F.; Marecek, J. F. *Synthesis* **1978**, 601.